7. EFFECT OF JET PITCH ANGLE ON SUPPRESSING FLOW SEPARATION

Compton and Johnston [15] investigated the strength and decay rate of a longitudinal vortex for seven cases of jet skew angle with a pitch angle of 45 degrees. They concluded that an optimal jet skew angle to strengthen the vorticity might be between 45 and 90 degrees to the downstream direction. However, a fixed pitch angle of 45 degrees was examined in their study. Therefore the effect of jet pitch angle on separation control and the subsequent downstream development of longitudinal vortices for various pitch angles were unknown. It is necessary that engineering design data (e.g., jet skew and pitch angles) should be provided for effective utilization because the beneficial effect of separation control is obtained only if the jets are pitched to a wall and skewed with respect to the freestream direction. In this chapter, we investigate the effect of jet pitch angle on suppressing flow separation and the downstream development of longitudinal vortices in three cases of jet pitch angles.

7.1 Experimental Method

Two freestream velocities U_0=6.5 and 11.1 m/s were investigated. The diffuser's divergence angle was set at 20 degrees. Figure 3.3 shows the configuration of jets and the coordinate system used to describe the flowfield. Three jets 2 mm in diameter were placed at the upstream of the divergent lower wall and their orifices were configured on the right side of the lower wall in the test section (viewed from upstream). The jets in this study were skewed at 90 degrees (θ =90

degrees) to the freestream direction (0 degree being downstream). The effect of jet pitch angle on suppressing flow separation was studied experimentally in three cases with the pitch angle set at 30, 45, and 60 degrees. The jet pitch angle can be changed by replacing the jet orifice unit shown in Fig. 3.4. Velocity measurements were carried out using an X-array hot wire probe. The hot wire probe was supported by a three-axis computer-controlled traverse unit. Streamwise velocity profiles were measured at Z=110 mm to avoid the effect of jet orifices and the downstream locations were chosen at X=40, 70, and 110 mm. The velocity measurements in a Y-Z plane were carried out at equal spaces of 5 mm, in the X and Y directions. Pressure recovery in the diffuser C_p was made in reference to the static pressure at two measurement points, in the upstream of the divergent portion (unstalled region) and in the divergent portion. Static pressure measurements were carried out at several stations in the divergent portion (see Fig. 3.13) using a differential pressure transducer which had the ability to measure very small differential pressure (0.01 mmAq).

7.2 Results and Discussion

7.2.1 Flow Visualization Results

The surface tuft method was used as the diagnostic technique to observe the effect of jet pitch angle of vortex generator jets on separation control. Tufts were put on the lower wall of the test section at every interval of 15 mm in the downstream direction at Z=125 and 140 mm. Figure 7.1 shows the surface flow in the divergent portion of the test section. The air flows from left to right of Fig. 7.1. For an unforced case flow separation is observed near the inlet of the divergent portion. It is seen from Fig. 7.1 that the separation point moves downstream by issuing jets. A pitch angle of 30 degrees or 45

degrees makes separation control more effective than the 60-deg case in the downstream direction.

7.2.2 Velocity Measurements in a *Y-Z* Plane

Streamwise vorticity of longitudinal vortices produced by the interaction between the jets and the freestream is shown in Fig. 7.2. In this study, we define the positive vortices in a *Y-Z* plane for vortices of clockwise-rotation when we view from upstream. For the 30-deg case negative vorticity due to the counter-rotating vortices produced on the upwash side of the longitudinal vortices are weaker than the positive vorticity at X=10 mm and therefore a pair of vortices of nearly equal strength does not exist at the measurement planes. In particular, the strength of negative vorticity is very weak compared with that of positive vorticity at X=70 and 110 mm. For the 45-deg case three pairs of vortices of nearly equal strength exist at X=10 mm. However, at X=70 and 110 mm a pair of vortices of nearly equal strength exits near Z=110 mm alone. Issuing jets at a pitch angle of 60 degrees have a tendency to produce strong counter-rotating vortices and consequently three pairs of vortices are maintained at the longer downstream location in comparison with the other cases. They move apart more rapidly from the lower wall than the other cases because of the velocity induced by a pair of vortices. In three cases of the jet pitch angle, the 30-deg case can keep the vortices at the location nearest to the lower wall in the downstream direction. The downstream development of longitudinal vortices for U_0=6.5 m/s is shown in Fig. 7.3. Comparing Fig. 7.2 with Fig. 7.3, we can see that the downstream development of longitudinal vortices in three cases of the jet pitch angle is quite similar to the U_0=11.1 m/s case. However, the vorticity for U_0=6.5 m/s decreases more rapidly in the streamwise direction than that for U_0=11.1 m/s because the longitudinal vortices are weaker than the U_0=11.1 m/s case.

For the 60-deg case three pairs of vortices have similarly upward

movements in the downstream direction. On the contrary, for the 45-deg and 30-deg cases the longitudinal vortex of positive vorticity on the left-side edge of Fig. 7.2 or 7.3 at X=110 mm is lifted away from the lower wall in comparison with the other vortices. For the 60-deg case longitudinal vortices keep their circular shape. However, for the 45-deg and 30-deg cases positive vortices do not keep their circular shape but rather become wider in the spanwise direction as they grow. Therefore, for the 45-deg and 30-deg cases the spanwise distance between two positive vortices becomes narrow and the negative vortices which exist between two positive vortices are split out in the vertical direction due to the interaction with the positive vortices on both sides. The negative vorticity decreases in the downstream direction and disappears at the longer streamwise distance. The upward movement of the positive vortex is suppressed because the split negative vortex exists above the positive vortex and no vortex pair is formed. The relationship between the vertical positions of the positive and negative vortices is also seen from Fig. 7.4 which shows the mean vorticity in the spanwise direction. For the 60-deg case the peak positive vorticity has the nearly equal vertical position of the peak negative vorticity. On the contrary, for the 45-deg and 30-deg cases the position of the peak negative vorticity in the vertical direction is higher than that of the peak positive vorticity. The positive vorticity on the left-side edge of Fig. 7.2 or 7.3 forms a vortex pair by the influence of negative vorticity which has not been split out. The positive vortex on the left-side edge of Fig. 7.2 or 7.3 exists at the higher vertical location in comparison with the other positive vortices due to the vortex pair. The movement of a vortex pair coincides with the results about the interaction between a vortex pair and a turbulent boundary layer shown by Pauley and Eaton [9].

Figures 7.5 and 7.6 show secondary flow velocities of longitudinal vortices. The secondary velocities toward the lower wall for the 60-deg case become weaker than those for the other cases because longitudinal vortices are lifted away from the lower wall. On the contrary, for the 30-deg and 45-deg cases the secondary flow toward the lower wall is observed near Y=−20 mm, and as a result the effective

suppression can be achieved (see Fig. 7.1). The suppression results from keeping longitudinal vortices near the lower wall and therefore the 60-deg case is inferior to the others regarding the control of boundary layer separation. In other words, it is desirable that longitudinal vortices are controlled in keeping their position near the lower wall. However, for the 45-deg case an upwash region is produced in a narrow spanwise region by a vortex pair at Z=110 mm (see Fig. 7.5(b) or 7.6(b)). The upwash makes ineffective the secondary flow toward the lower wall.

7.2.3 Separation Effect versus Jet Pitch Angle

The pressure recovery from an unforced case C_{pdf} is defined as

$$C_{pdf} = C_{p_{VR}} - C_{puf} \quad , \tag{7.1}$$

where C_p is expressed in Eq. (2.6), subscript uf and VR indicate the unforced case and issuing jet case, respectively. Figure 7.7 shows the distribution of pressure recovery along the wall static pressure holes. It is seen from Fig. 7.7 that the effective pressure recovery is obtained in order of a pitch angle of 30, 45, and 60 degrees for the same VR. In particular, comparing the 30-deg case with the 45-deg case for VR=5.6 at X=110 mm, the high pressure recovery is obtained for the 30-deg case. Figure 7.8 shows the downstream decay of the maximum positive vorticity. The vorticity is strong in order of a pitch angle of 30, 45, and 60 degrees at X=10 mm. However, the vorticity for the 60-deg case is stronger than that for the 45-deg case at X=110 mm. This means that considerable things for separation control are not the strength of longitudinal vortices solely. As mentioned above, for the effective separation control it is necessary that longitudinal vortices exist near the lower wall and the secondary flow which can transport high momentum fluid of the freestream toward the lower wall is produced. For the 30-deg case longitudinal vortices are strong and can keep their positions near the lower wall. Therefore, for the 30-deg

case the effective separation control can be achieved in lower VR in comparison with the 45-deg and 60-deg cases.

Figure 7.9 shows the streamwise velocity profiles at X=110 mm. For the 30-deg and 60-deg cases the near-wall velocity increase in the divergent portion is observed. The near-wall velocity increase for the 30-deg case is larger than that for the 60-deg case because the strong secondary flow toward the lower wall is produced by the longitudinal vortices which exist near the lower wall in comparison with the 60-deg case (see Fig. 7.2 or 7.3). On the other hand, for the 45-deg case near-wall velocity increase is not observed. This is because the streamwise velocity measurements are carried out just at the plane where the upwash occurs (see Fig. 7.9).

7.2.4 Suppression Effect in the Downstream Direction

Figure 7.10 shows flow visualization results at X=200 mm for the 30-deg and 45-deg cases. The visualization images indicate that the suppression effect for the 45-deg case persists further downstream and wider in the spanwise direction than that for the 30-deg case. Figure 7.11 shows the distribution of pressure recovery in the divergent portion. The value of C_{pdf} for the 30-deg case is higher than that for the 45-deg case at X=110 and 160 mm. However, the value of C_{pdf} for the 45-deg case is higher than that for the 30-deg case at X=200 and 250 mm. This means that the effective pressure recovery for the 45-deg case is obtained over a longer downstream distance in comparison with that for the 30-deg case.

Figures 7.12 and 7.13 show vorticity contours and secondary flow vectors measured at X=200 mm, respectively. Comparing Fig. 7.12(a) with Fig. 7.12(b), we see that the downstream development of longitudinal vortices for a pitch angle of 45 degrees is different from that for a pitch angle of 30 degrees. For the 30-deg case three pairs of

vortices become a single vortex. On the other hand, for the 45-deg case three pairs of vortices are degenerated to a counter-rotating vortex pair in the downstream direction. Because for the 45-deg case the negative vortex of nearly equal strength to the positive one is produced near the injection point of the jet flow. On the contrary, for the 30-deg case the negative vortex is weaker than the positive one near the same location. Comparing Fig. 7.13(a) with Fig. 7.13(b), we can see that the secondary velocities for the 30-deg case become stronger in the spanwise direction than in the vertical direction at the region between Z=120 mm and Z=140 mm. On the other hand, for the 45-deg case the secondary velocities toward the lower wall are strong at the same spanwise region under the influence of a pair of vortices. This is because the secondary flow of the positive vortex in the spanwise direction is interrupted by the secondary flow of the negative vortex at the upper and slant location of the positive vortex and the flow in the spanwise direction is directed toward the lower wall.

Accordingly, in the 30-deg case separation control is made effectively because longitudinal vortices keep their location near the lower wall and become stronger than in the other cases. However, the secondary velocities toward the lower wall become weaker over a longer streamwise distance due to the existence of a single vortex, and as a result the spanwise region in which the suppression effect can be obtained decreases at the longer streamwise direction. On the contrary, for a pitch angle of 45 degrees longitudinal vortices are degenerated to a counter-rotating vortex pair and the suppression effect persists further downstream.

7.3 Conclusions

From the present experimental study for discussing the effect of jet pitch angle of vortex generator jets on separation control, the following conclusions were drawn:

1. The effective separation control using vortex generator jets is accomplished by keeping the location of longitudinal vortices near the lower wall.

2. For a pitch angle of 60 degrees, longitudinal vortices move apart more rapidly from the lower wall than the other cases, and hence the 60-deg case is inferior to the others regarding the control of boundary layer separation.

3. For the 45-deg case, three pairs of vortices are degenerated to a counter-rotating vortex pair in the downstream direction, and as a result the secondary velocities toward the lower wall become strong and the suppression effect persists further downstream. However, if an upwash occurs at the spanwise location, the suppression effect of flow separation could not be achieved in the upwash region.

4. In the 30-deg case, separation control is made effectively because longitudinal vortices become stronger than in the other cases and keep their location near the lower wall. In other words, this case enables us to perform separation control at a lower jet flow rate. However, the region in the spanwise direction which gives suppression effect decreases in the downstream direction in comparison with the 45-deg case because three pairs of longitudinal vortices become a single vortex over a longer streamwise distance and the downward secondary flow becomes weaker near the lower wall.

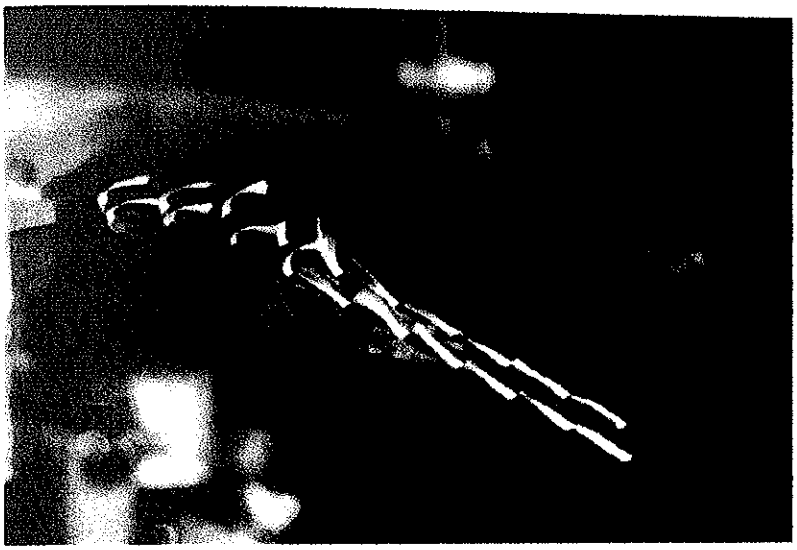

(a) Unforced

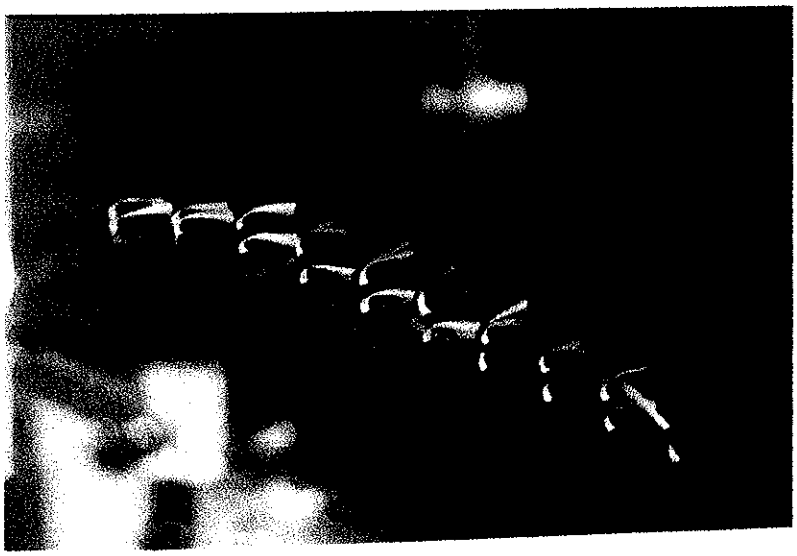

(b) ϕ =30 deg

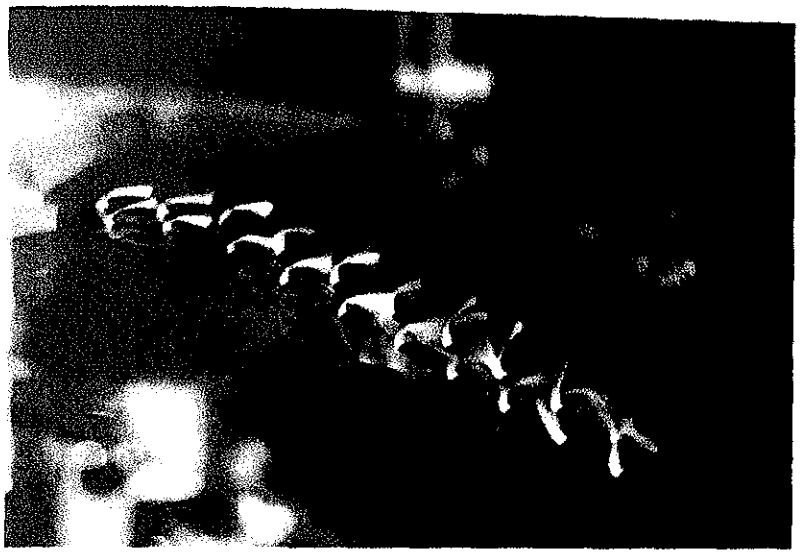

(c) ϕ =45 deg

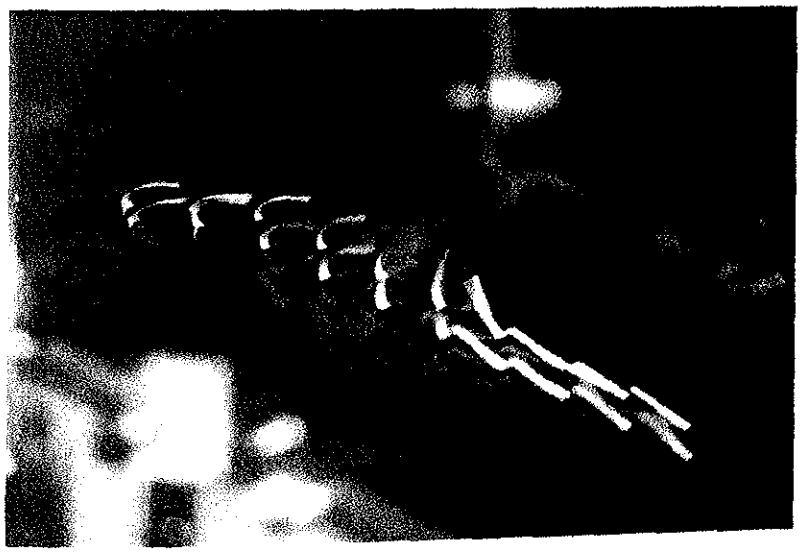

(d) ϕ =60 deg

Figure 7.1 Surface flow in divergent portion of the test section (U_0=11.1 m/s, VR=9.5).

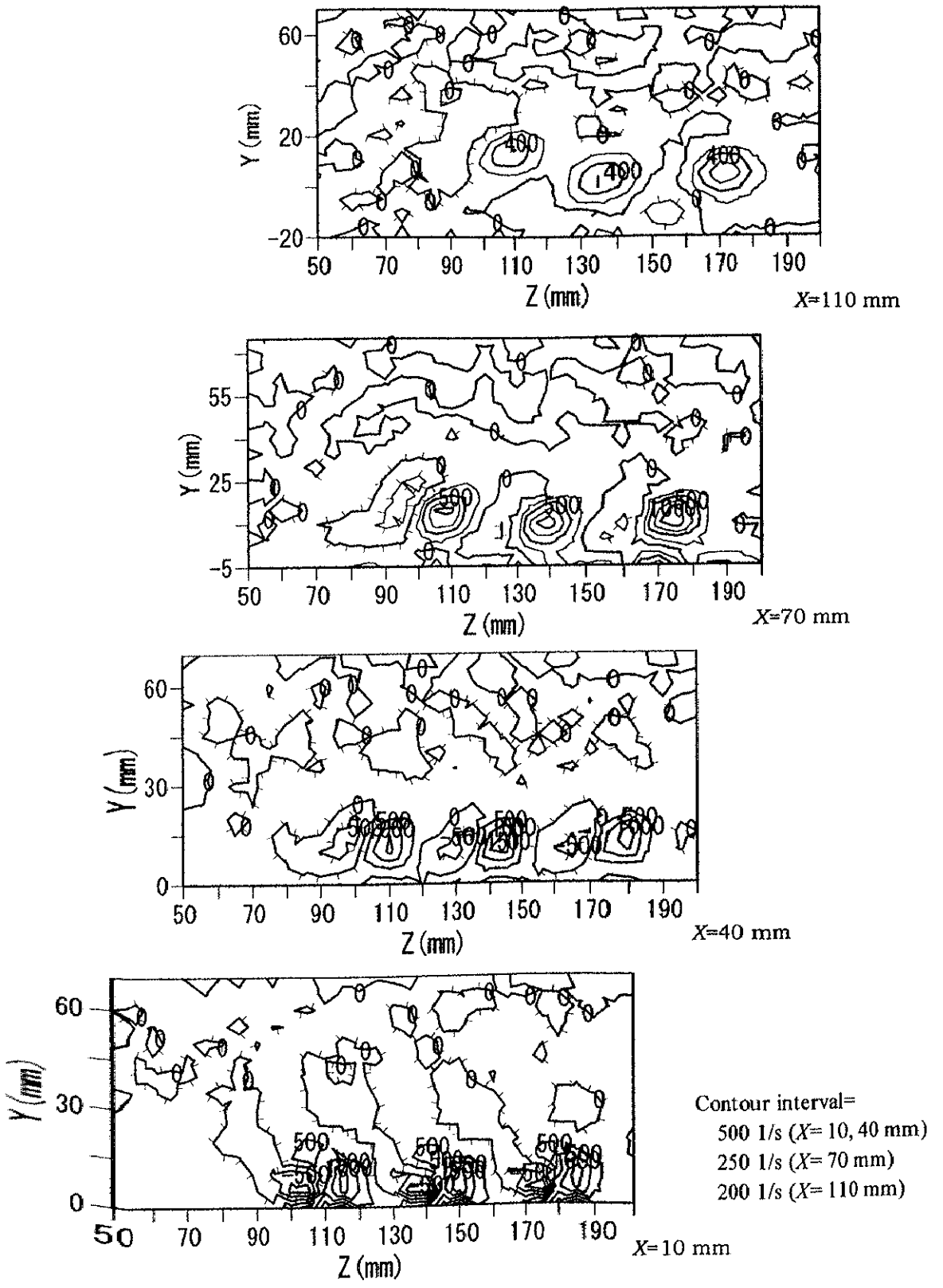
Y (mm)
Z (mm)
X=110 mm
X=70 mm
X=40 mm
X=10 mm
Contour interval=
500 1/s (X= 10, 40 mm)
250 1/s (X= 70 mm)
200 1/s (X= 110 mm)

(a) ϕ =30 deg

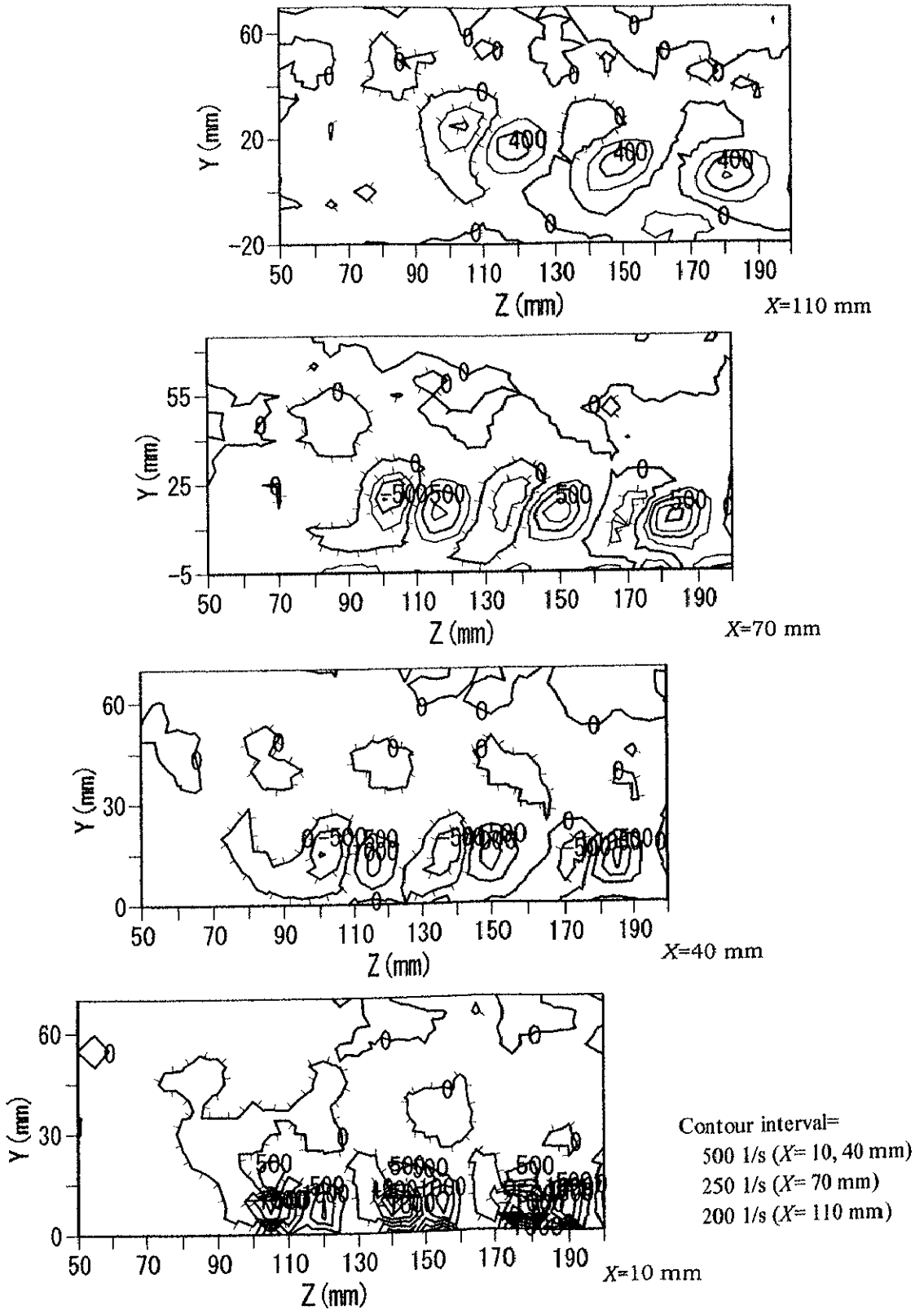
Y (mm)
Z (mm)
X=110 mm
X=70 mm
X=40 mm
X=10 mm
Contour interval=
500 1/s (X= 10, 40 mm)
250 1/s (X= 70 mm)
200 1/s (X= 110 mm)

(b) ϕ =45 deg

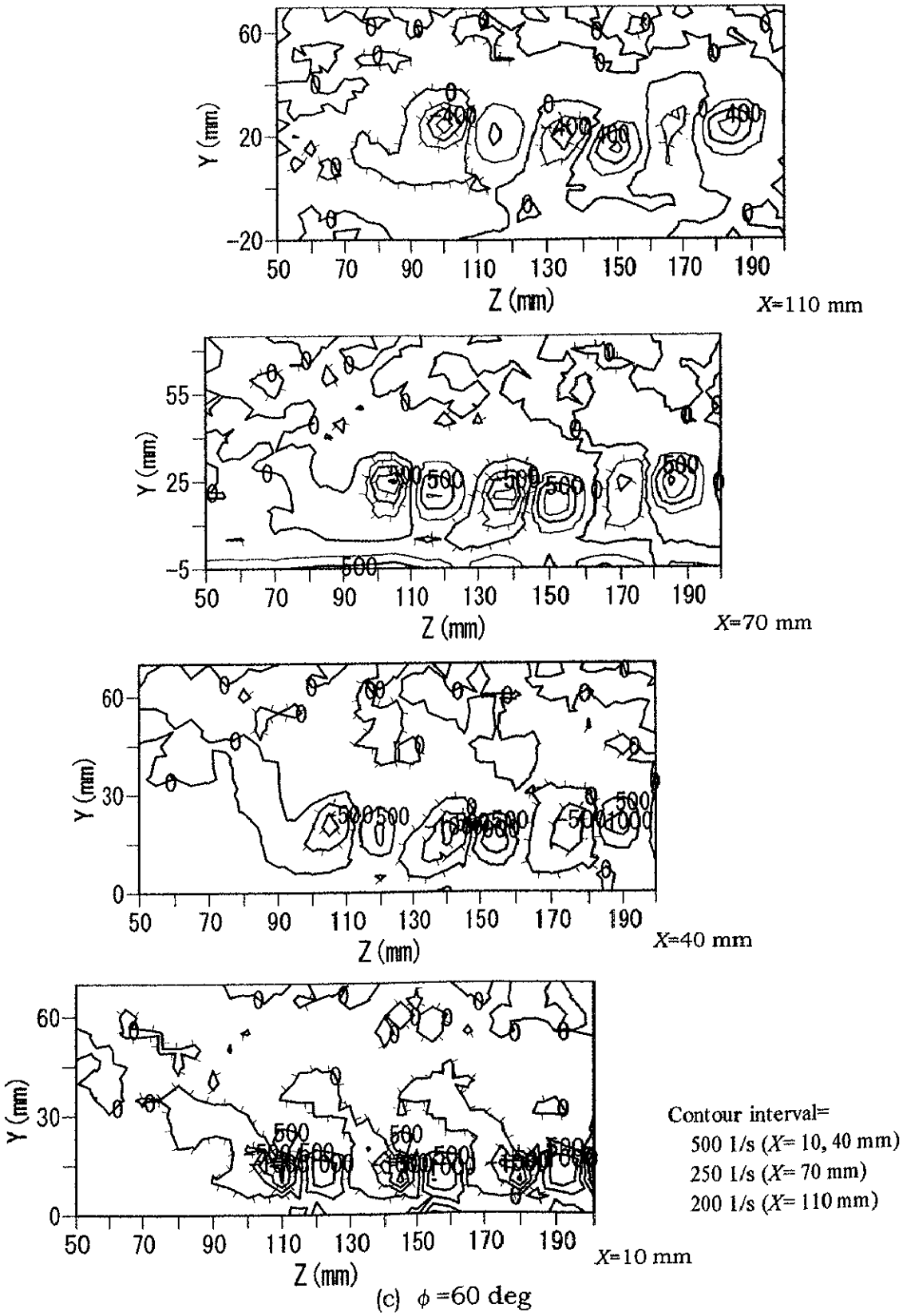

(c) ϕ =60 deg

Figure 7.2 Contours of streamwise vorticity (U_0=11.1 m/s, VR=9.5). Decorated lines denote negative vorticity.

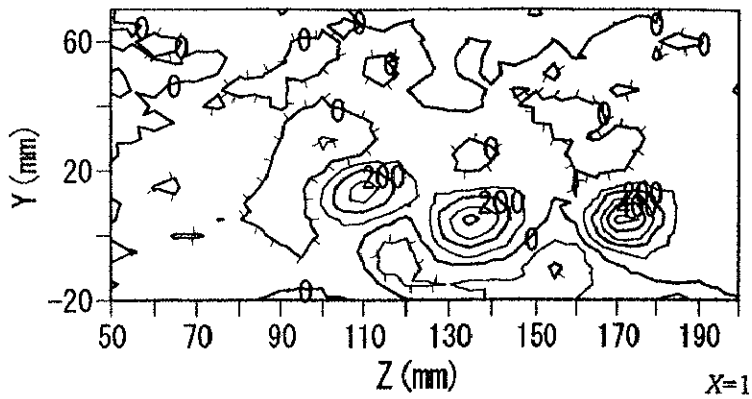

X=110 mm

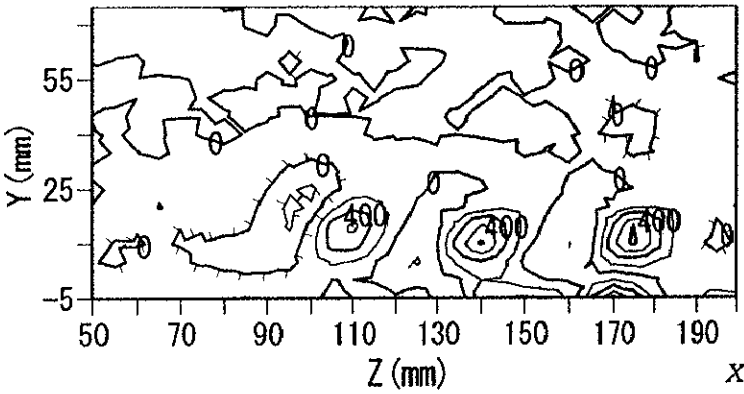

X=70 mm

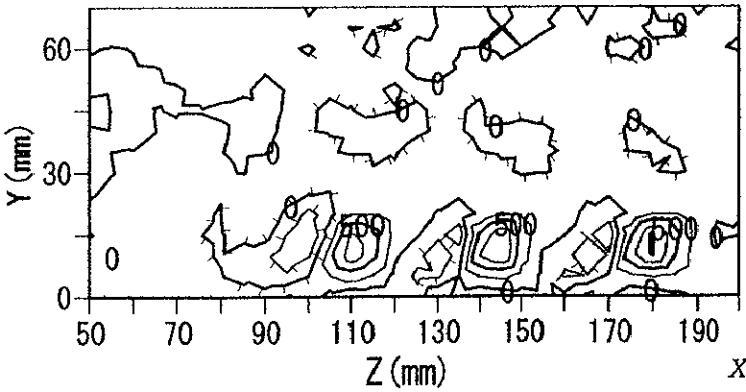

X=40 mm

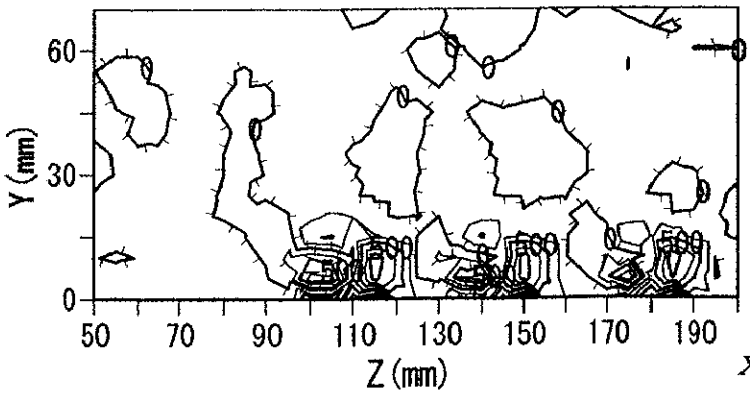

X=10 mm

Contour interval=
500 1/s (*X*= 10, 40 mm)
250 1/s (*X*= 70 mm)
200 1/s (*X*= 110 mm)

(a) ϕ =30 deg

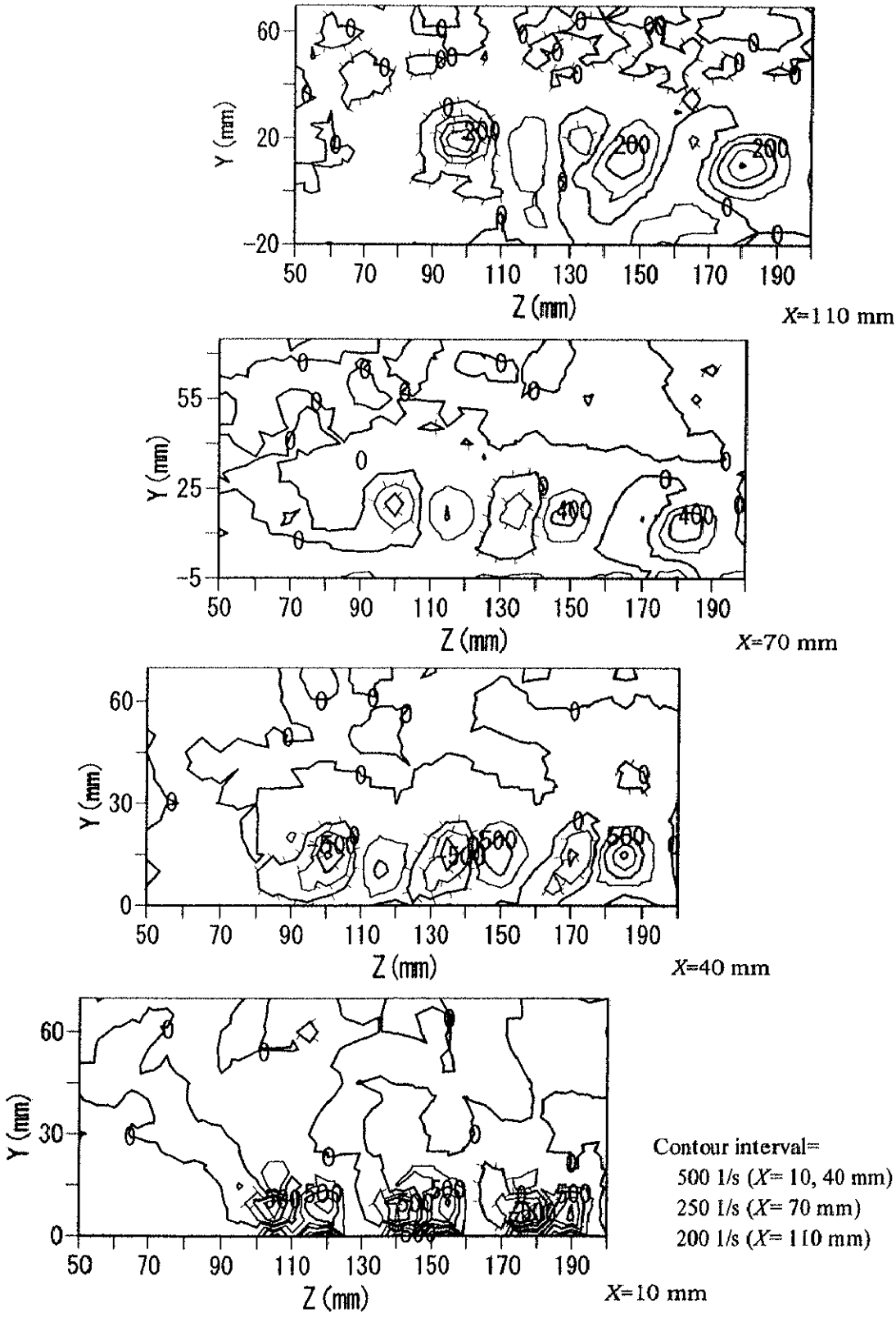
Y (mm)
Z (mm)
X=110 mm
X=70 mm
X=40 mm
X=10 mm
Contour interval=
500 l/s (X= 10, 40 mm)
250 l/s (X= 70 mm)
200 l/s (X= 110 mm)

(b) ϕ =45 deg

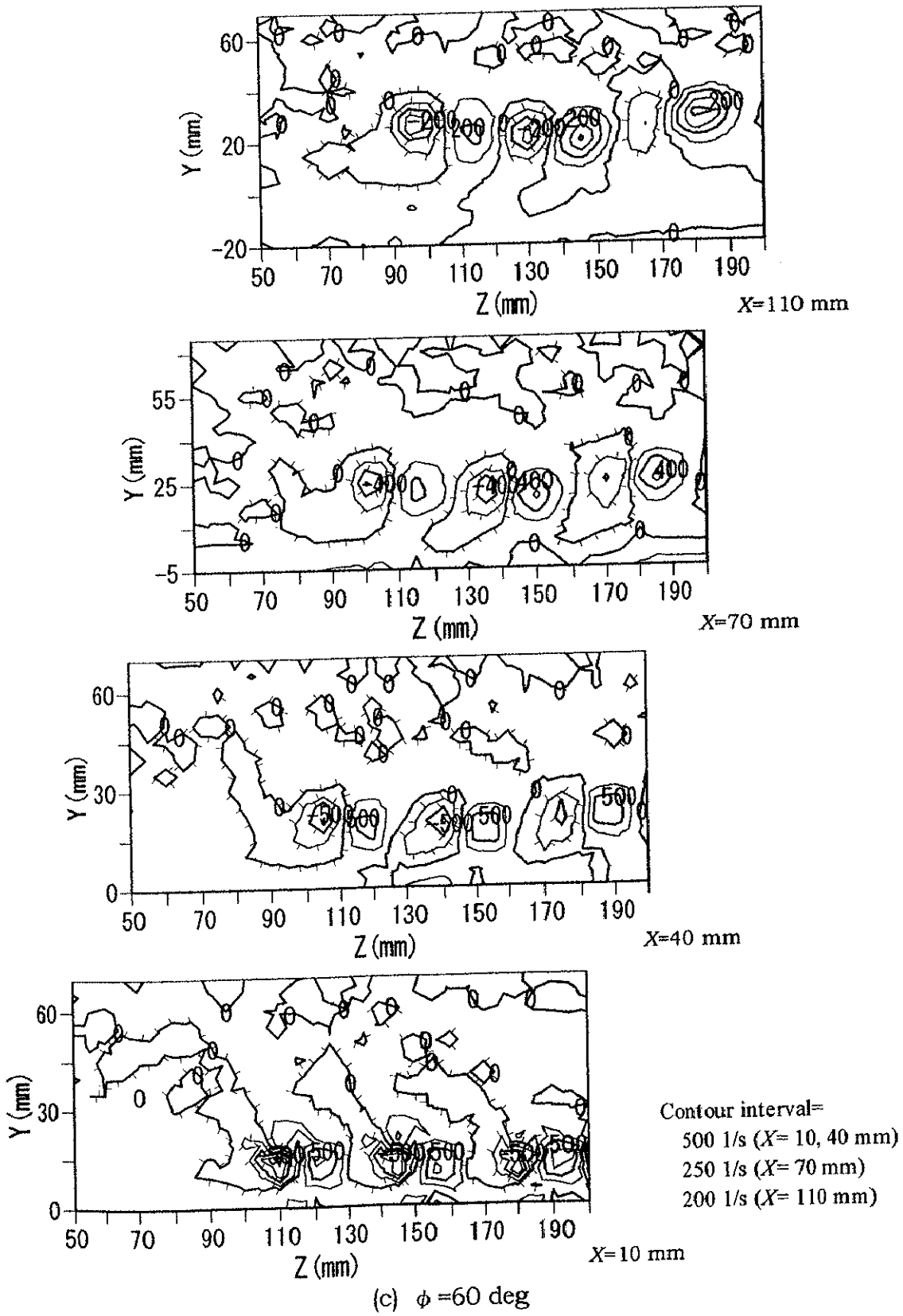

(c) ϕ =60 deg

Figure 7.3 Contours of streamwise vorticity (U_0=6.5 m/s, VR=9.5). Decorated lines denote negative vorticity.

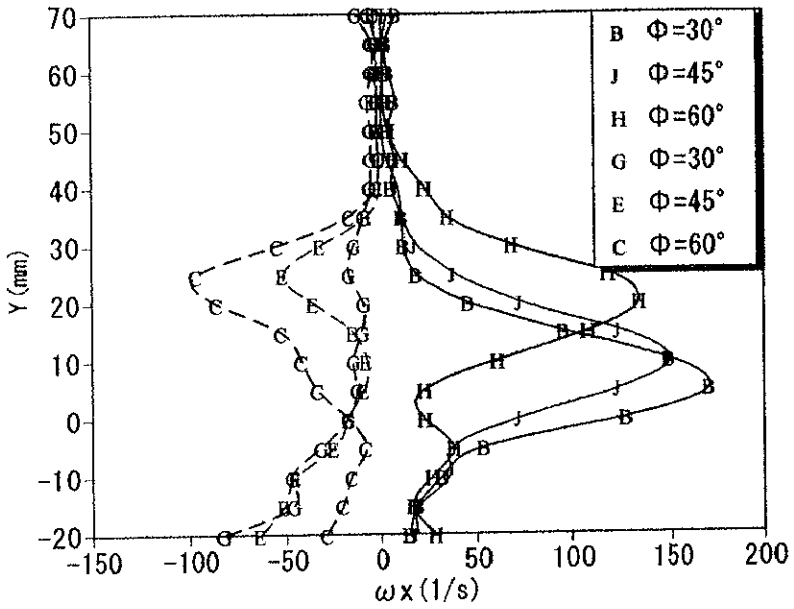

(a) U_0=11.1 m/s, VR=9.5

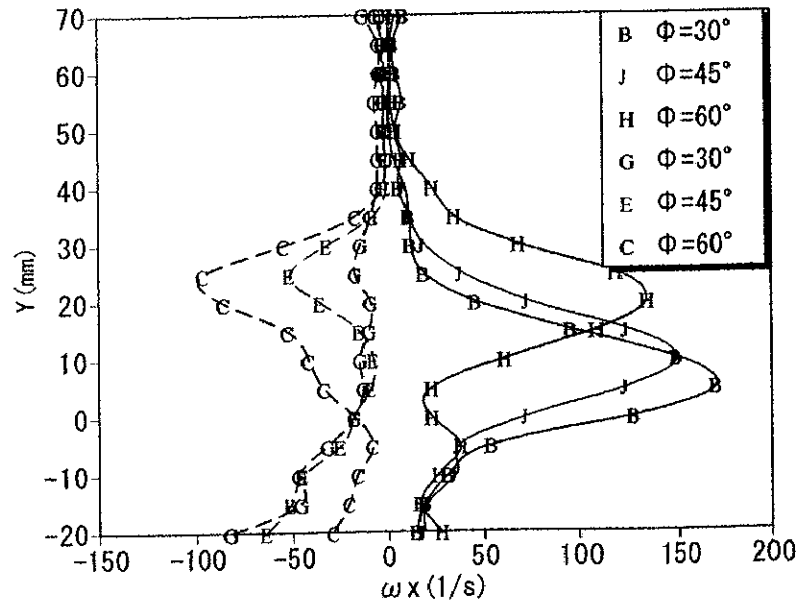

(b) U_0=6.5 m/s, VR=9.5

Figure 7.4 Mean vorticity in spanwise direction at X=110 mm. Open symbols denote negative vorticity.

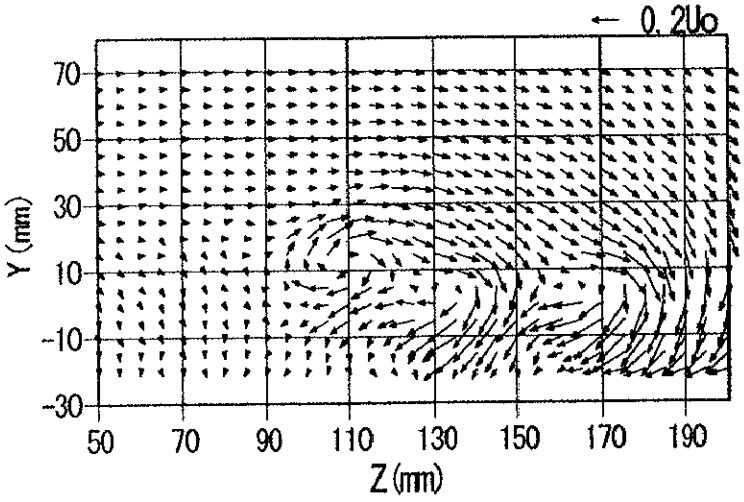

(a) ϕ =30 deg

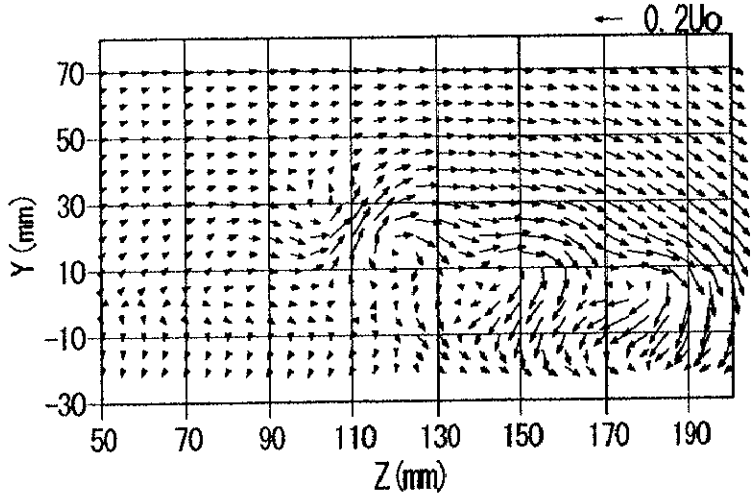

(b) ϕ =45 deg

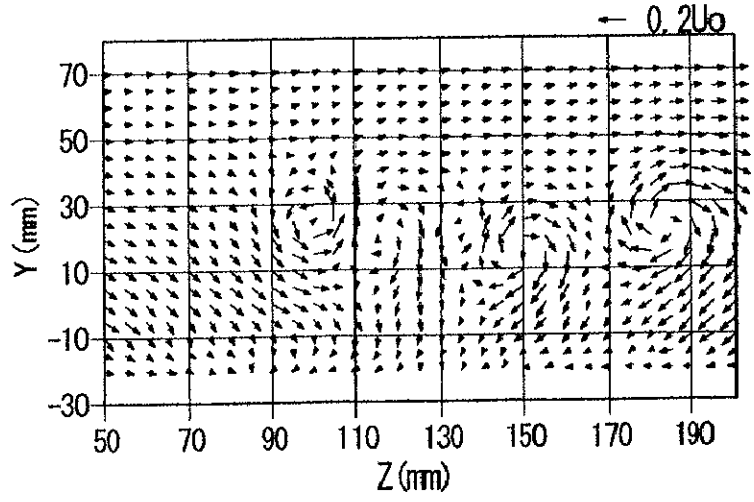

(c) ϕ =60 deg

Figure 7.5 Secondary flow vectors at X=110 mm (U_0=11.1 m/s, VR=9.5).

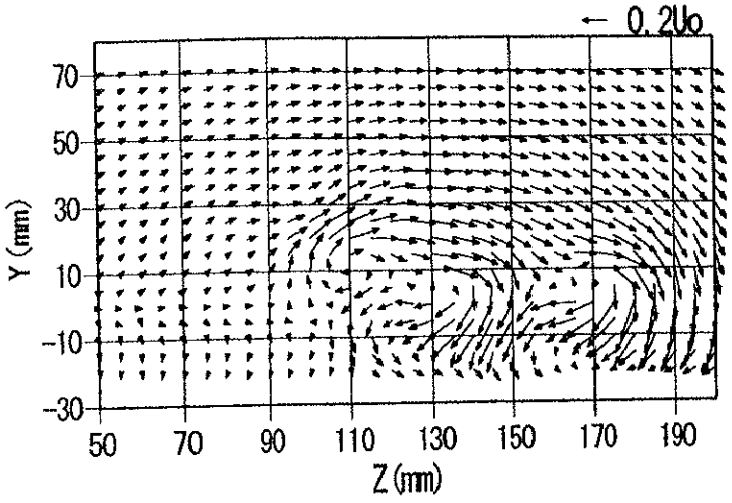

(a) ϕ =30 deg

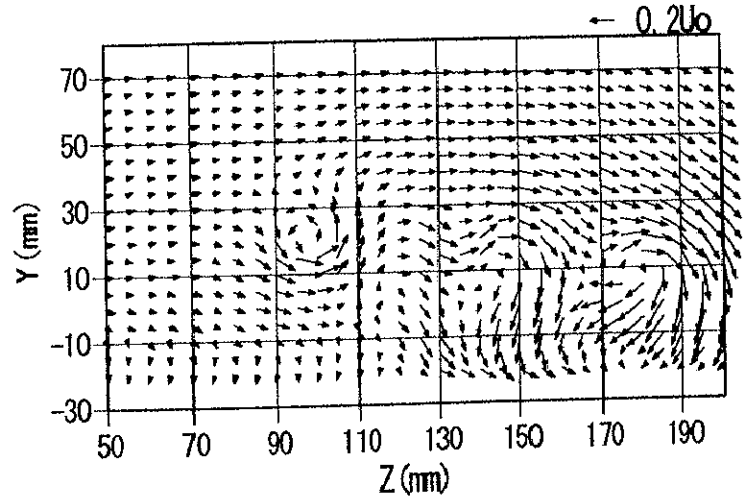

(b) ϕ =45 deg

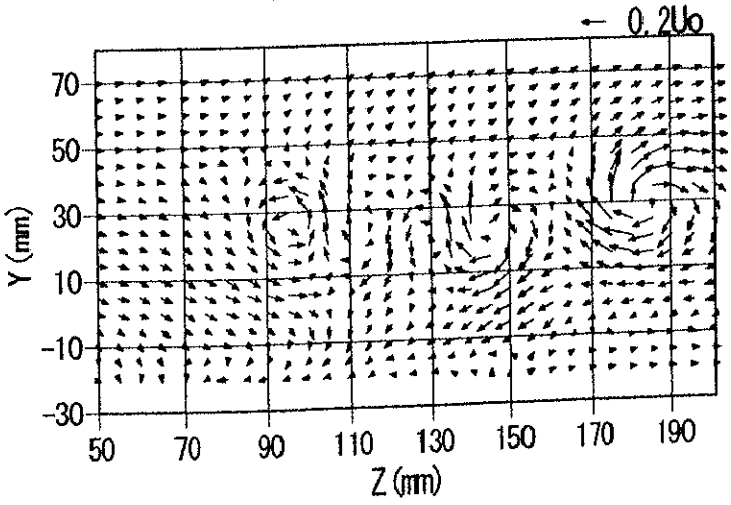

(c) ϕ =60 deg

Figure 7.6 Secondary flow vectors at X=110 mm (U_0=6.5 m/s, VR=9.5).

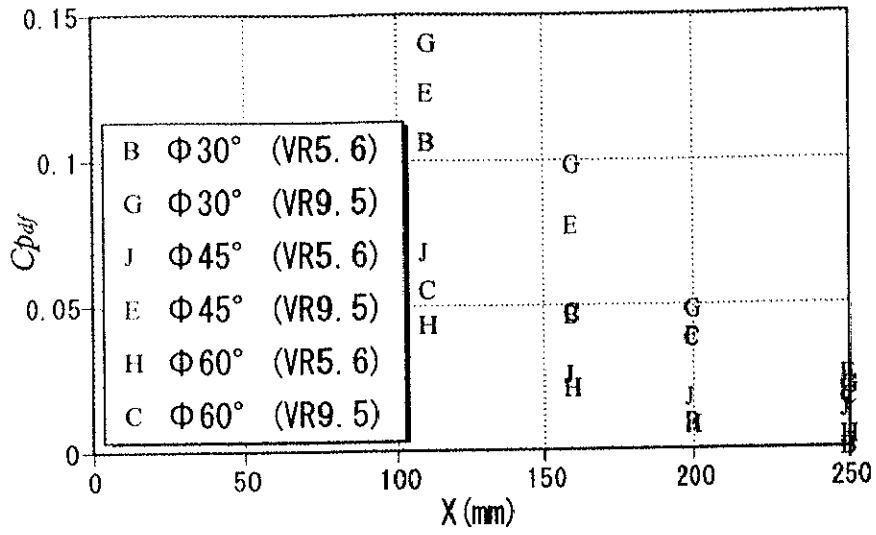

Figure 7.7 Distribution of pressure recovery along the wall static pressure holes of divergent portion (U_0=11.1 m/s).

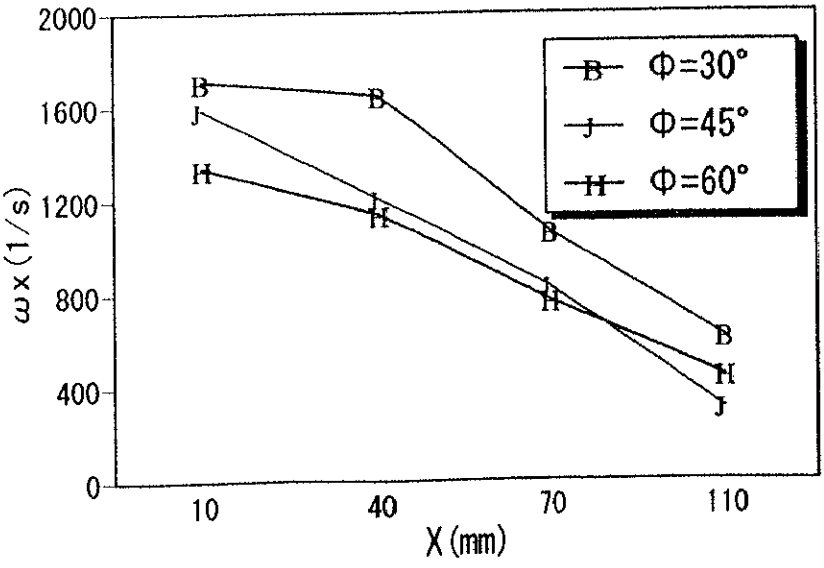

Figure 7.8 Effect of pitch angle on the downstream decay of maximum positive vorticity (U_0=11.1 m/s, VR=9.5).

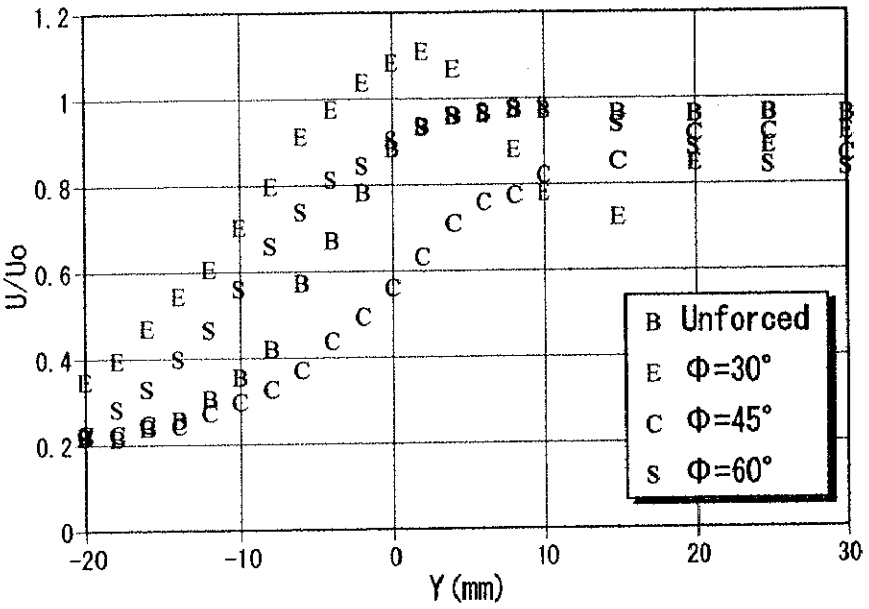

(a) U_0=11.1 m/s, VR=9.5

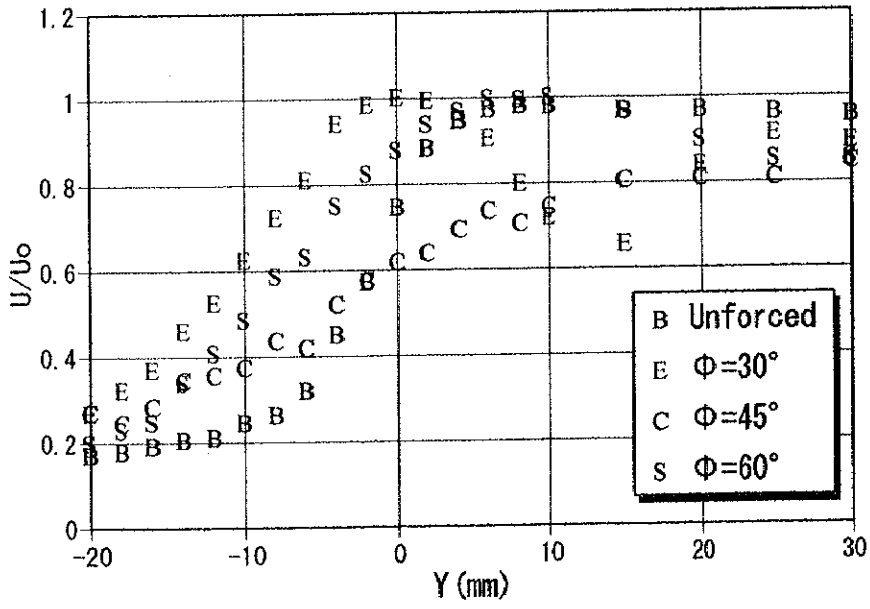

(b) U_0=6.5 m/s, VR=9.5

Figure 7.9 Streamwise velocity profiles at X=110 mm.

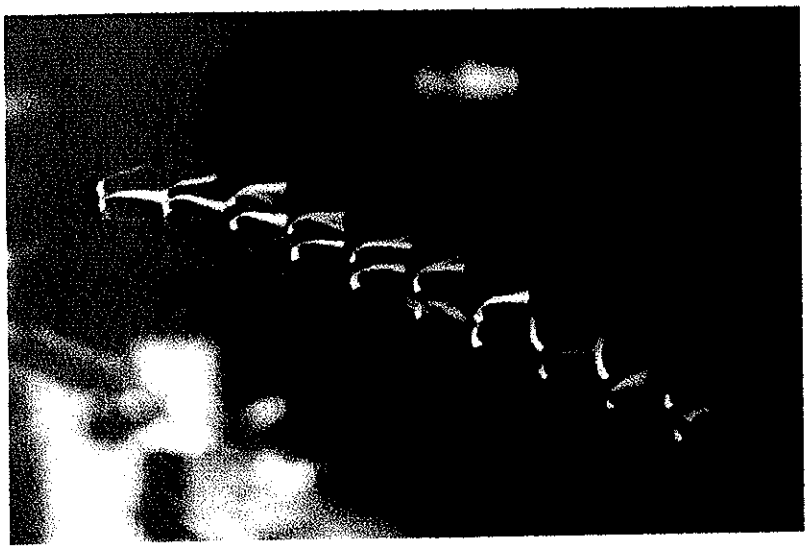

(a) ϕ =30 deg

(b) ϕ =45 deg

Figure 7.10 Surface flow in divergent portion of the test section (U_0= 11.1 m/s, VR=14).

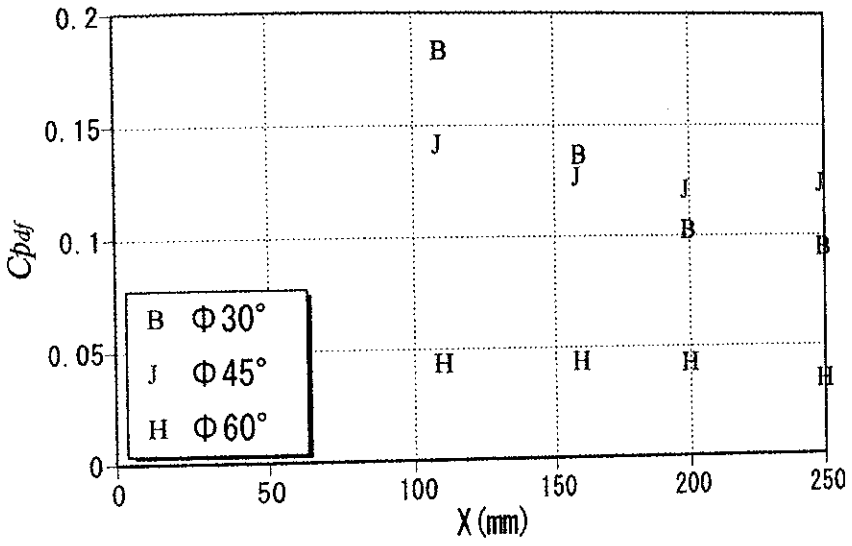

Figure 7.11 Distribution of pressure recovery along the wall static pressure holes of divergent portion (U_0=11.1 m/s, VR=14).

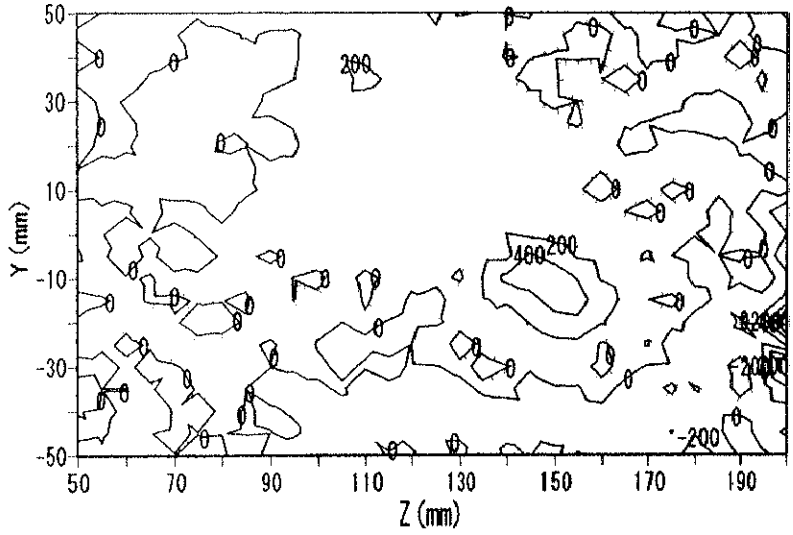

(a) ϕ =30 deg (Contour interval=200 1/s)

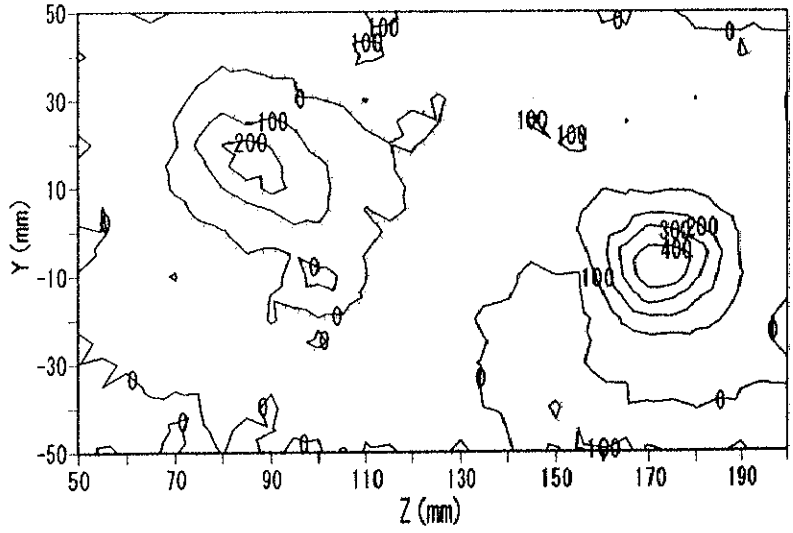

(b) ϕ =45 deg (Contour interval=100 1/s)

Figure 7.12 Contours of streamwise vorticity at X=200 mm (U_0=11.1 m/s, VR=14). Decorated lines denote negative vorticity.

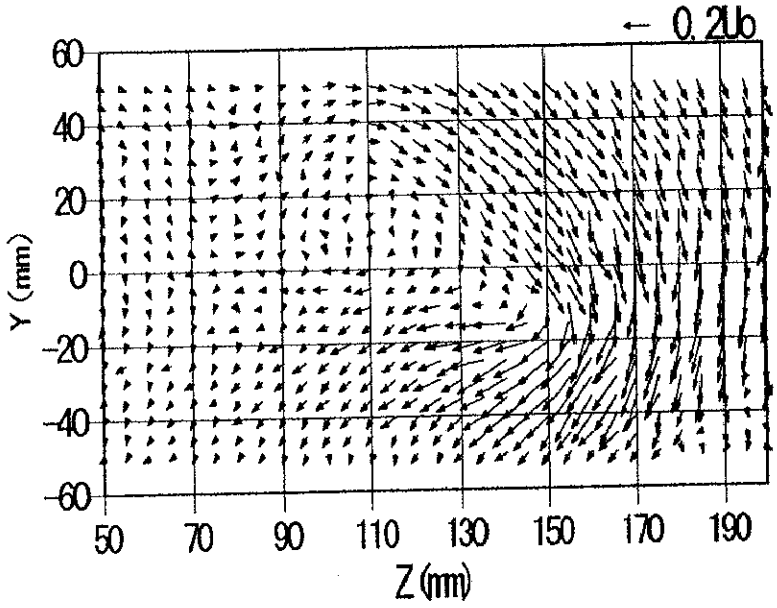

(a) ϕ =30 deg

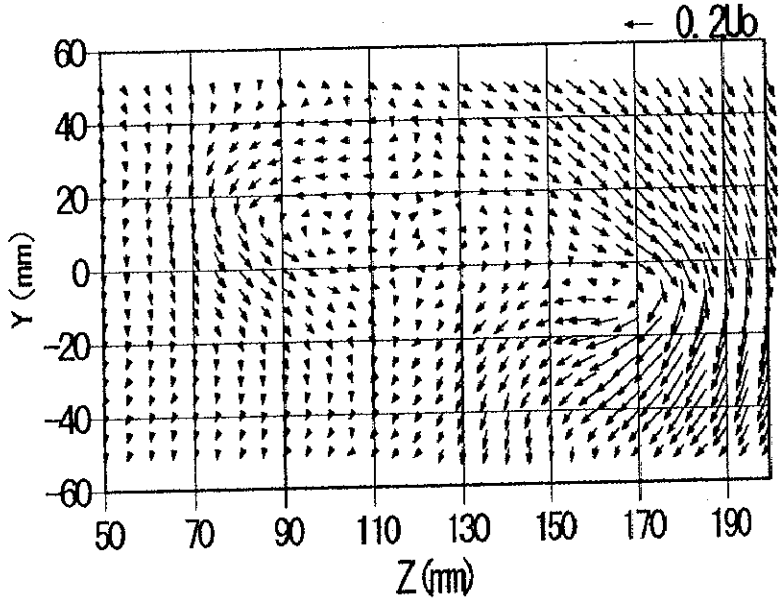

(b) ϕ =45 deg

Figure 7.13 Secondary flow vectors at X=200 mm (U_0=11.1 m/s, VR=14).